Chapter 6

Glaze analysis of shards and plates

Probing pigments successfully through the glaze using micro-Raman spectroscopy for the first time necessitates the detailed study of the glaze through which the incident laser beam travels and the Raman scattered radiation passes before detection. Among the properties that will be investigated are: (1) type of glaze: for example SiO_2 or SnO_2; (2) element type and relative concentration in the glaze; (3) possible melting temperature of the glaze based on the methods of Colomban and co-workers;[1-5] and (4) level and type of technology employed by the manufacturers. Based on the results from the analysis, comparisons will be made with samples whose manufacturers and, to some extent, manufacturing technology are known. Differences and/or similarities can then be used to group or exclude samples according to likely manufacturing technology and therefore origin.

6.1. Glaze analysis method

The method of glaze analysis that was used in this work is that already employed by Colomban and co-workers.[1-5] The Raman spectrum of the glass/glaze network is composed of broad bands around 500 cm^{-1} and 1000 cm^{-1}. The band at 500 cm^{-1} has been attributed to ν_2 bending vibrations of the isolated SiO_4 unit, while that around 1000 cm^{-1} is composed largely of the stretching vibrations of the coupled ν_1 and ν_3 vibrations.[5] It is deduced that the highly connected SiO_4 tetrahedral units in the SiO_4 network will have high Raman band intensity from the bending vibrations, as illustrated with arrows in Figure 6.1.1.

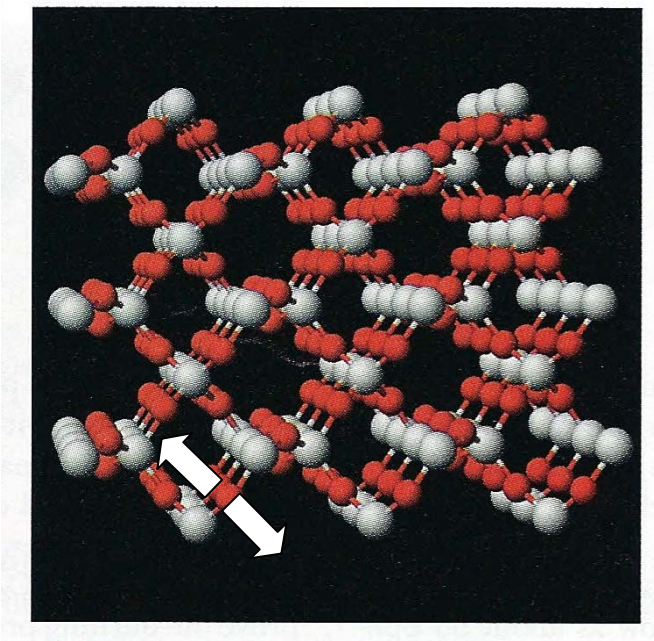

Figure 6.1.1. In highly connected SiO_4 tetrahedral units, such as in the SiO_2 network, the bending vibrations illustrated here with white arrows are most intense and are associated with the 500 cm^{-1} envelope in the Raman spectrum (Silicon atoms are the grey spheres and the red spheres are those of oxygen atoms.) [The Figure was obtained and modified from Kotz, J.C. and Treichel, P. Chemistry and Chemical Reactivity, 4th Ed, Harcourt Brace College Publishers, Orlando, Florida USA.]

When fluxing agents are added to the amorphous glaze, such as calcium, sodium and other fluxing agents that are used to lower sintering temperatures, this out-of-axis bending vibration is reduced. However, the stretching Si-O vibration that is associated with the 1000 cm^{-1} region is not affected. It is this difference that led Colomban[6] to define an index of polymerisation, I_p, such that, $I_p = A_{500}/A_{1000}$, where A_i is the area under the Raman band centred at wavenumber i. It follows that a relationship can be developed between the glass/glaze sintering temperature and the glass/glaze composition.

Since the Raman spectra of porcelain glazes are also generally dominated by broad bands around 500 cm^{-1} and 1000 cm^{-1}, which are associated with v_2 bending vibrations and the coupled ν_1 and ν_3 Si-O stretching vibrations of the isolated tetrahedra, we focused our analysis in this region. In the deconvolution of the silicate stretching envelope (ca 700 – 1300 cm^{-1}) one can define five components within this region, namely Q_o (originating from an isolated tetrahedron), Q_1 (tetrahedra linked by a common oxygen atom, Si_2O_7), Q_2 (tetrahedra linked by sharing two oxygen atoms, $3Si_3O_9$ with n-tetrahedral cycles), Q_3 (tetrahedra linked by sharing three oxygen atoms) and Q_4 (as it appears in pure SiO_4).[6-9] These Q_n values are found to have characteristic Raman signatures and should assist in determining the degree of polymerisation of the silicate network and hence the type and concentration of the fluxing agents used.

6.2. Application to blue and white porcelain glaze

Fluorescence in Raman spectroscopy as applied to the study of glazed ceramic artifacts greatly affects the spectral assignment because it can mask spectra collected from the glaze and/or pigments in the sample. In this case the fluorescence emanates from the glaze of the artifacts and is attributed largely to the presence of impurities[10] and the degree of porosity of the glaze under study.[11] The use of a confocal set-up in Raman microscopy ensures that mainly the spectrum from the focus point is obtained.[12-14] This allows the collection of scattered radiation from volumes of the order of one cubic micron at the focus point, thereby discriminating between the glaze spectra and those from the interfacial region (glaze/ceramic). This region is usually composed of decorative pigments and other colouring agents which are then detected through the intervening glaze.[13,14]

Figure 4.2.1. and Figure 4.2.2 show the glaze depth profile spectra (raw data), illustrating the systematic approach adopted towards obtaining interfacial pigment

Raman spectra. One of the questions raised pertains as to whether the clear ceramic/glaze interfacial pigment spectra so obtained[13,14] are dependent on the glaze type as a function of the glaze composition and/or of the processingtemperature? The glaze on the samples already studied was analysed in order to answer this question.

In addition, the information obtained was used to further compare and contrast Ming porcelain artifacts and shards of archaeological origin. Intact Ming dynasty porcelain plates and a tile shard from the Citadel of Algiers were also studied and comparisons were made. A well-documented method developed by Colomban and co-workers[7,15,16] for the analysis of glaze/glass was used in the analysis of the glaze. Since the glaze thicknesses of the samples studied are between 0.1 mm and 0.4 mm, laser powers of 40 mW and 20 mW respectively were required.[13]

6.2.1. Samples

The samples used in the glaze studies are the same as those used for the pigment studies. The pigments on these samples have been studied in depth and the results have been reported.[13,14] Figure 6.1.2 shows the sample set, made up of Ming samples A and B, unknown samples of archaeological origin C, D and F, sample E of Meissen origin and the Citadel tile, sample G. In addition, the Ming plates (samples H and I of the Hongzhi (1488–1505) and Wanli (1573–1620) imperial periods respectively) were also studied.

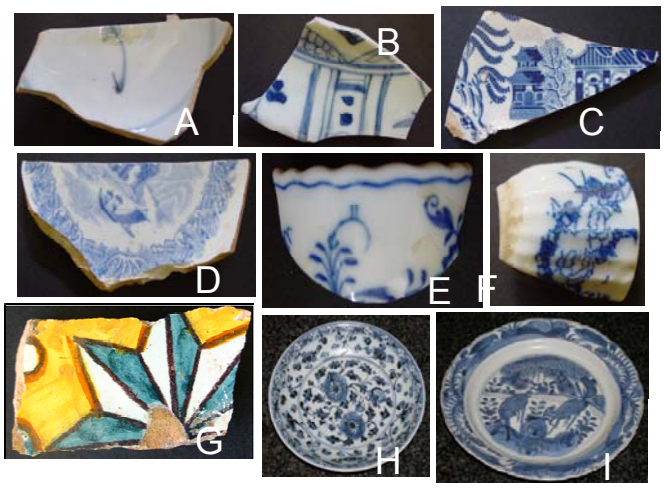

Figure 6.2.1.1. These sets of shards and intact plates are those that were used for the glaze analysis. Samples A and B are Ming shards, C, D and F are of archaeological origin, E is of Meissen origin, H and I are intact museum collection pieces and G is the tile shard from the Citadel of Algiers

The glaze thicknesses were estimated with a ruler and the measurements were made on the broken edges where this was possible. The samples were used as received with no further preparation, apart from wiping with methanol to clean the glaze surfaces where necessary.

6.2.2. Raman and EDX measurements

A Dilor Raman machine (Dilor XY multi-channel spectrometer) with a spectral resolution of about 2 cm^{-1}, equipped with a liquid nitrogen-cooled CCD detector was used in the Raman measurements. An Olympus confocal microscope in a 180^{o} backscattering configuration was attached to the spectrometer. 50X and 100X windows were used for the silicate glazes found on the blue and white porcelain samples and Olympus objective lenses with long focal lengths were used. Integration times were typically between 120 and 300 seconds, with two to three accumulations in each spectrum.

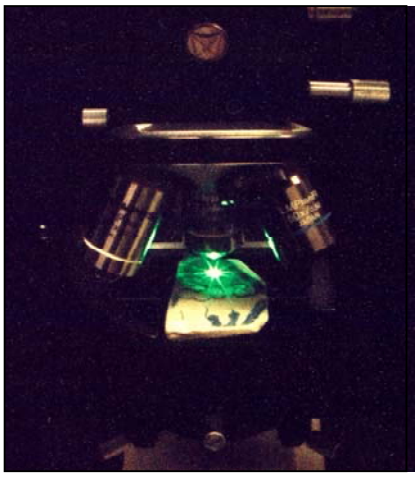

Figure 6.2.2.1. The Figure illustrates the position of the shard in a normal horizontal position for probing the glaze directly. This position is also ideal for probing the ceramic/glaze interface through the glaze on the shards.

The excitation radiation was 514.5 nm wavelength supplied by an Innova 300 argon ion laser with the power set typically at between 0.5 mW and 40 mW. The laser powers are reported as measured at the sample, the target being the glaze and not the pigment in those samples that had some pigment exposed to the surface. Data acquisition, baseline corrections and spectra processing were carried out with LabSpec® software (Jobyn Yvon, Horiba Group).

Peak fitting was undertaken with Origin® software (Microcal Software Inc.). The EDX measurements were carried out with a JEOL JSM – 5800LV scanning electron microscope operated at low vacuum, with an accelerating voltage of 20 kV. The use of low vacuum eliminated the need for gold sputtering to enhance surface conductivity.

6.2.3. Results on sample glazes

The raw data Raman spectra collected from the glaze surfaces to the interfacial region of the porcelain samples are shown in Figure 4.2.1. and Figure 4.2.2., where used in the glaze analysis studies. Only the glaze surface spectra of the samples were used in these studies in order to compare the various glaze properties.

It was also found that relatively high fluorescence emanated from the intact Ming plates (samples H and I) and both the Ming shards (samples A and B) show intermediate and mutually similar relative fluorescence intensities. This is in contrast to the unknown archaeological shards (samples C, D and F) and the Meissen shard (sample E), which showed relatively little fluorescent activity, making it easier to probe through the glaze. Visually, the unknown shards of archaeological origin and the Meissen shard show a clear transparent glaze as compared with the Ming porcelain (shards and intact plates), which have a tint of white inside the glaze due to the higher density of bubbles or air pockets in the glaze. This high density of bubbles in the glaze qualitatively correlates with increased fluorescence. In the case of porcelain glaze, fluorescence is usually attributed to organic or inorganic contaminants in the open pores within the glaze.[8]

Since the high laser powers used on these blue and white samples is expected to have cleaned the glaze surfaces of any organic impurities, the relative degrees of fluorescence intensity on these samples is most likely due to inorganic impurities, the glaze composition and/or the microstructure rather than that from surface-borne organic impurities.

Organic or inorganic impurities trapped inside the glaze could also give rise to fluorescence. The glaze spectra from all the samples were similarly treated by a

two-point correction to remove the slope and move the baseline to zero. The baseline corrections were effected by LabSpec® software.

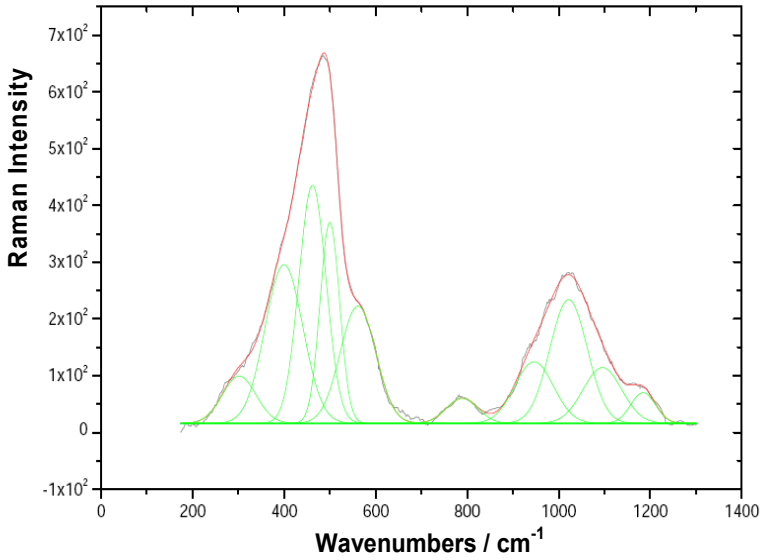

Figure 6.2.3.3. Representative deconvolution results from glaze spectra (514.5 nm wavelength radiation; 50X objective lens). Figure 4.2.1. (a) was used in the illustrated deconvolution.

The same smoothing functions within the same spectral window between 200 cm-1 and 1300 cm-1 were used to prepare spectra before a Gaussian function was applied in a peak-fitting procedure using the Origin® curve-fitting software to produce the spectra shown in Figure 6.2.3.3. Since the index of polymerisation (I_p = A_{500}/A_{1000}) is correlated with the processing temperature and composition of glassy silicates,[6] this parameter was calculated from the Raman signature of the various glaze types and used to predict the glaze properties. The data extracted from Figure 6.2.3.3 are shown in Table 6.2.3.1.

Table 6.2.3.4. Peak maximum as obtained from the deconvolution process of the glaze spectra for the various blue and white samples and the calculated index of polymerisation (I_p). The νQ_n values are indicated in cm^{-1}

Sample	νQ_0	νQ_1	νQ_2	νQ_3	νQ_4	I_p
Ming A	803	937	1006	1061	1134	1.4
Ming B	798	951	1022	1089	1162	2
Unknown C	794	938	1007	1083	1161	2.7
Unknown D	789	945	1011	1093	1174	2.3
Unknown F	795	939	1012	1086	1166	4
Meissen E	798	964	1026	1093	1165	1.8
Plate H (Hongzhi)	782	919	975	1040	1118	2.1
Plate I (Wanli)	788	946	1021	1095	1184	2.4
Tile G						0.3

The index of polymerisation from Table 6.2.3.1 is also presented graphically in Figure 6.2.3.4, which gives values for the I_p per sample, showing the spread of the index of polymerisation (I_p) for the various samples. At I_p = 0.3 for the tile glaze, it may indicate sintering temperatures of < 600 ^oC for this tile shard.[6] The rest of the samples show I_p values above 1.3 which could indicate sintering temperatures well above 1 000 ^oC.

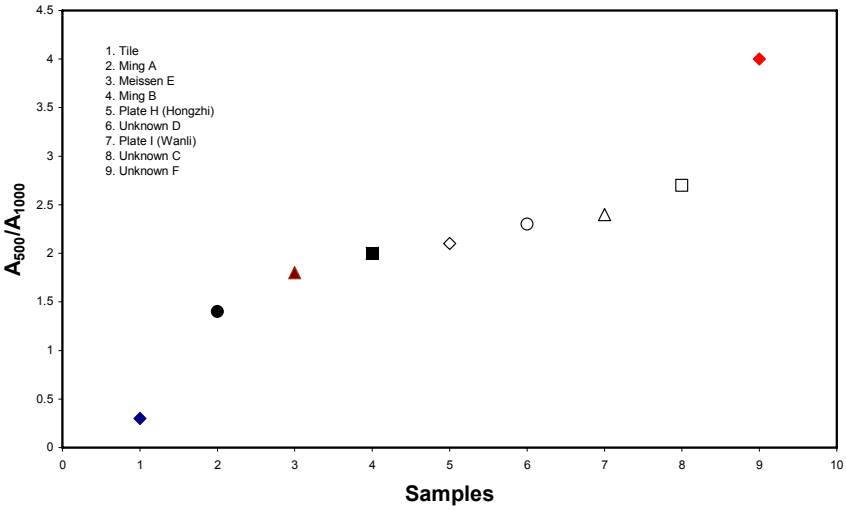

Figure 6.2.3.4. Plot of the A_{500}/A_{1000} ratio (index of polymerisation, I_p) of the various samples. This ratio has been found to correlate closely with the sintering temperature of the glaze

Differentiation between lead-based and alkali-based glaze types is possible,[6,9] while processing temperature determinations follow directly from consideration of the degree of connectivity of the SiO_4 polymeric units, which are determined from the relative Raman intensities of the Si-O bending (500 cm^{-1}) and stretching (1000 cm^{-1}) modes.[7]

The EDX results (Table 6.2.3.2) also show the weight of Pb in the tile glaze to be approximately 53%, the highest in the set of samples.

Table 6.2.3.2. EDX data listing the main elements in the glaze of the selected samples

Element (Wt%)	Ming A	Ming B	Unknown C	Unknown D	Unknown F	Meissen E	Tile G
Na	0.15	1.03	0.99	0.83	1.06	0.64	0.14
Mg	0.23	0.07	0.56	0.29	0.07	1.05	0.2
Al	9.74	8.8	8.41	8.53	7.86	11.32	2.01
Si	57.97	62.49	52.64	47.98	66.52	64.16	28.5
K	8.49	9.7	7.52	5.99	12.73	7.28	3.7
Ca	20.32	14.52	8.3	16.89	6.32	12.86	0.65
P	0.09	0	0.1	0.11	0.07	0.18	0.09
S	0	0	0	0	0	0	0
Cl	0.27	0.11	0	0.07	0.09	0	0.12
Ti	0.35	0.16	0.38	0.3	0.09	0.13	0.07
Fe	2.24	3.08	1.54	0.59	1.89	2.38	0.44
Co	0.15	0.03	0.52	0.34	0	0	0
Pb	0	0	19.03	18.09	3.35	0	52.71
Sn	n.d.	n.d.	n.d.	n.d.	n.d.	n.d.	9.78

(n.d. = Not determined)

These glaze types contain lead, alkaline earth metals and alkali metals acting as fluxing agents that lower the glass transition temperature of the glassy networks. Both the Ming samples (A, B, H and I) and the unknown samples show I_p values far above 1.3, corresponding to glass transition temperatures of about 1 000 ^oC or more.[7] Again, the EDX results confirm the dominance of Ca over Pb in the Ming samples. There is no detectable lead content in the Ming samples. Note that only shards, and not intact plates, were used in the EDX studies due to the small size of our EDX instrument sample chamber.

The Meissen sample (E), with an I_p of 1.3, also corresponds to Ca-based glazes (Pb-poor), with Raman-predicted glass transition temperatures of about 1 000 ^oC or more (see also Table 6.2.3.2 for EDX data confirming the Meissen shard glaze composition). These results are also consistent with those of other Meissen porcelain studies.[16] The depth profiling method can also be used to estimate the glaze thickness on intact ceramic artifacts. The glaze thicknesses of the samples are listed in Table 6.2.3.3, as estimated by direct measurement with a ruler (in the

case of the broken shards) and by using a laser beam (all listed samples) to reach the ceramic/glaze interface.

Table 6.2.3.3. Glaze thicknesses of the samples studied as determined by direct measurement using a ruler and by approximate location of the ceramic/glaze interface using a laser beam

	Ming A	Ming B	Unknown C	Unknown D	Unknown F	Meissen E	Tile G	Plate H (Hongzhi)	Plate I (Wanli)
Thickness (mm)	0.4	0.4	0.1	0.1	0.1	0.2	n.d.	-	-
Thickness (μm)	450	424	124	128	116	240	n.d.	394	420

(n.d. = Not determined).

6.4 Conclusion

The glaze types on all the blue and white ceramic samples studied in this work ranged from Ca-based (samples A, B and E) to Pd-dominated (samples C, D and G) and had glass transition temperatures ranging from high (~1 000 ^{o}C or more) to low (~600 ^{o}C). All the types were studied successfully by using the depth profiling method. The SnO_2-dominated glaze type of the tile shard from the Citadel of Algiers was also successfully probed using this method. The variation in the value of the index of polymerisation ($I_p = A_{500}/A_{1000}$), which is known to be closely correlated with the degree of polymerisation of the silicate network and is affected by the type and concentration of fluxing agents in the glaze, shows that the samples are vastly different and have had different manufacturers. This result further supports the conclusions reached in an earlier study,[13] namely that the two groups of shards (Ming and archaeological) are not likely to have a common origin. Using the depth profiling method, we are also able to approximate the glaze thickness on intact ceramic pieces.

6.5 References

1. Colomban, P., Liem, N.Q., Sagon, G., Tinh, H.X. and Hoành, T.B. *J. Cult. Heritage*. 2003, **4**, 187.

2. Colomban, P., Milande, V. and Le Bihan, L. *J. Raman Spectrosc*. 2004, **35**, 527.

3. Colomban, P. and Truong C. *J. Raman Spectrosc.* 2004, **35**, 195.

4. Prinsloo, L.C. and Colomban, P. *J. Raman Spectrosc.* 2008, **39**, 79.

5. Prinsloo, L.C., Wood, N., Loubser, M., Verryn, S.M.C. and Tiley, S. *J. Raman Spectrosc*. 2005, **36,** 806.

6. Colomban, P. *J. Non-Cryst. Solids*. 2003, **323**, 180.

7. Colomban, P., March, G., Mazerolles, L., Karmous, T., Ayed, N., Ennabli, A. and Slim, H. *J. Raman Spectrosc*. 2003, **34**, 205.

8. Liem, N.Q., Thanh, N.T. and Colomban, P. *J. Raman Spectrosc*. 2002, **33**, 287.

9. Colomban, P. and Treppoz, F. *J. Raman Spectrosc*. 2001, **32**, 93.

10. Osticioli, I., Zoppi, A. and Castelluci, M. *J. Raman Spectrosc.* 2006, **37**, 974.

11. Colomban, P. *Mater. Res. Soc. Symp. Proc*. 2005, **852E,** 008.4.1.

12. Huang, P.V. *Vibrational Spectrosc*. 1996, **11**, 17.

13. Kock, L.D. and de Waal, D. *J. Raman Spectrosc*. 2007, **38**, 1480.

14. Kock, L.D. and de Waal, D. *Spectrochim. Acta*. 2008, **71A**, 1348.

15. Colomban, P., Tournie, A. and Bellot-Gurlet, L. *J. Raman Spectrosc*. 2006, **37,** 841.

16. Colomban, P. and Milande, V. *J. Raman Spectrosc.* 2006, **37**, 606.

Chapter 7

Overall conclusion

Raman spectroscopy analysis of underglaze pigments of porcelain of archaeological origin was undertaken. The samples that were used in the study form four categories: (1) shards of unknown origin from archaeological sites around Pretoria, kept by the National Cultural History Museum, and shards of Ming origin also from the National Cultural History Museum in Pretoria; (2) one shard of Meissen origin from Germany; (3) intact plates from the Ming dynasty, as well as one intact plate of unknown origin; and (4) a tile shard from the Citadel of Algiers.

Raman spectroscopic analysis was undertaken, with additional techniques being used to complement the Raman work, namely energy-dispersive X-ray spectrometry (EDX) and X-ray powder diffractometry (XRD). Synthesis methods were also used to aid in the characterisation of pigments. Reference compounds were synthesised and their analyses were compared and contrasted with those it was intended to identify on the artifacts.

The overall study proved very successful in the characterisation of all the pigments on all the samples that were chosen for the study. Firstly, cobalt blue was positively identified on all of the blue and white porcelain shards and plates, except on the unknown intact museum plate on which an olivine-type blue pigment was identified. Comparative studies between the Ming blue pigment and the blue pigment on the pieces of unknown origin were used to look for differences between these two groups that could be used to indicate differences in place of origin or manufacture.
For instance, the use of amorphous carbon to darken the blue pigment on the unknown shards is not known to have been common among the Ming manufacturers.

Secondly, the use of white (hence pure) anatase to whiten the surface of the porcelain artifact before the application of the glaze is also not found to be common among the Ming manufacturers.

These differences could be used by archaeologists in solving some of the mysteries emanating from excavated porcelain shards from archaeological sites.

Studies of pigments on the tile shard from the Citadel of Algiers also proved very successful. All pigments were identified and characterised, except for the blue pigment on the tile for which Raman spectroscopy was unable to yield a spectrum. However, a cobalt blue spectrum was eventually obtained from a crevice on the surface after repeated attempts to probe the surface. It has been shown elsewhere that cobalt ions dissolved in the glaze do not give a distinct Raman signature but do give a brilliant blue colour. The ancient ternary (Pb-Sn-Sb) pigment that was also identified on the yellow section of the tile was successfully characterised and for the first time – a Pb-O vibration for this pigment was assigned at 127 cm^{-1}.

The method of glaze depth profiling uniquely employed during these studies proved very useful, especially in probing underglaze pigments on all the blue and white porcelain (shards and plates), and can now be used in further studies to compare and contrast pigments from museum pieces with those of archaeological origin. This technique will certainly complement the analytical techniques that are employed by archaeologists.

Overall, these studies proved very successful. However, due to the small sample group, further work should continue along the same lines in this young field in order to further establish Raman spectroscopy as a routine analysis technique in art and archaeology.